AGU ADVANCING EARTH AND SPACE SCIENCES

Geophysical Research Letters

RESEARCH LETTER
10.1029/2024GL108715

Key Points:

- 3.05 and 2.9 Ga granitoids derived from juvenile crust are identified in the SW Yangtze Block
- Global crust rejuvenation occurred across the Paleo-to Mesoarchean transition
- This period of rejuvenation resulted from the effects of peak mantle temperatures

Supporting Information:

Supporting Information may be found in the online version of this article.

Correspondence to:

Y.-G. Xu and W. Wang,
yigangxu@gig.ac.cn;
wwz@cug.edu.cn

Citation:

Lu, G.-M., Xu, Y.-G., Wang, W., Spencer, C. J., Huang, G., & Roberts, N. M. W. (2024). Continental crust rejuvenation across the Paleo-Mesoarchean transition resulted from elevated mantle geotherms. *Geophysical Research Letters*, *51*, e2024GL108715. https://doi.org/10.1029/2024GL108715

Received 6 FEB 2024
Accepted 26 MAR 2024

Author Contributions:

Conceptualization: Gui-Mei Lu, Yi-Gang Xu, Wei Wang, Nick M. W. Roberts
Data curation: Gui-Mei Lu, Christopher J. Spencer, Nick M. W. Roberts
Formal analysis: Gui-Mei Lu, Christopher J. Spencer, Guangyu Huang, Nick M. W. Roberts
Funding acquisition: Gui-Mei Lu, Yi-Gang Xu, Wei Wang
Methodology: Gui-Mei Lu
Software: Gui-Mei Lu, Guangyu Huang
Supervision: Yi-Gang Xu, Wei Wang
Visualization: Gui-Mei Lu, Guangyu Huang
Writing – original draft: Gui-Mei Lu

Continental Crust Rejuvenation Across the Paleo-Mesoarchean Transition Resulted From Elevated Mantle Geotherms

Gui-Mei Lu[1], Yi-Gang Xu[1], Wei Wang[2], Christopher J. Spencer[3], Guangyu Huang[4], and Nick M. W. Roberts[5]

[1]State Key Laboratory of Isotope Geochemistry, Guangzhou Institute of Geochemistry, Chinese Academy of Sciences, Guangzhou, China, [2]State Key Laboratory of Geological Processes and Mineral Resources, School of Earth Sciences, China University of Geosciences, Wuhan, China, [3]Department of Geological Sciences and Geological Engineering, Queen's University, Kingston, ON, Canada, [4]State Key Laboratory of Lithospheric Evolution, Institute of Geology and Geophysics, Chinese Academy of Sciences, Beijing, China, [5]Geochronology and Tracers Facility, British Geological Survey, Nottingham, UK

Abstract The increase in initial Hf isotopes identified in early Mesoarchean detrital zircon is commonly interpreted as a reflection of the geodynamic transition from stagnant-lid to mobile-lid tectonics. However, given the lack of petrogenetic context, interpreting detrital zircon may lead to spurious conclusions. In this contribution, we use zircon U-Pb-Hf-O isotopic and bulk rock compositions of newly identified 3.05–2.9 Ga granitoids from the SW Yangtze Block to posit petrogenesis within an isotopically juvenile magmatic system. A statistical analysis of these data with a global igneous zircon Lu-Hf isotopic compilation reveals an increase in average initial radiogenic Hf isotopes during the Paleoarchean to Mesoarchean transition. We posit that the Earth's continental crust underwent a global rejuvenation across the Paleo-Mesoarchean transition. This rejuvenation can be explained by an independently observed increase in mantle temperatures resulting from mantle thermal evolution and does not require a change in tectonic style.

Plain Language Summary In this study, we explore the Earth's continental crust evolution before 3.0 billion years ago, a period characterized by limited preserved ancient rocks. We focus on zircon from igneous rocks, which provides a more reliable petrogenetic record than detrital zircon. Our study challenges the widely observed increase in detrital zircon initial Hf isotopes during the Paleo-to Mesoarchean transition, often interpreted as a shift in tectonic regimes. We present new data from 3.05 to 2.9 billion-year-old granitoids in the Yangtze Block, suggesting isotopically juvenile magmatic activity. Statistical analysis of a global database of igneous zircon Hf isotopes reveals a state-shift increase in $\varepsilon Hf_{(t)}$ across the Paleo-to Mesoarchean transition, indicating global crustal rejuvenation at that time. Contrary to prevailing theories, we propose that this rejuvenation can be attributed to elevated mantle temperatures, challenging the notion of a significant geodynamic change during this period. Our findings emphasize the need to consider mantle thermal evolution in understanding continental crust growth on early Earth.

1. Introduction

The nature and evolution of Earth's continental crust before 3.0 Ga remain elusive, largely due to the relative scarcity of preserved ancient (>3.0 Ga) rocks. The use of detrital zircon helps to mitigate this issue, not only as they preserve more continuous records than the extant igneous rocks over Earth's history, but also as they can provide multiple records through analyses of several isotope systems (e.g., U-Pb-Hf-O) (Roberts & Spencer, 2014; W. Wang et al., 2023). Despite these advantages, owing to the absence of petrogenetic information on the source rocks, the reliability of the detrital zircon record may be hindered by hidden ancient lead loss, which results in artificially young ages and erroneous initial Hf isotopes (Guitreau & Blichert-Toft, 2014; Vervoort & Kemp, 2016).

It has been widely noticed that a step increase in detrital/igneous zircon initial Hf isotopes (expressed as $\varepsilon Hf_{(t)}$) from sub-chondritic to supra-chondritic values across the Paleo-to Mesoarchean transition for various cratonic blocks (e.g., Slave, Rae, Wyoming, Pilbara, Singhhum, Kalahari, and Greenland) (Bauer et al., 2020; Kirkland et al., 2021; Naeraa et al., 2012; Neil et al., 2023; Reimink et al., 2019). These unique isotopic signals were

Writing – review & editing: Gui-Mei Lu, Yi-Gang Xu, Wei Wang, Christopher J. Spencer, Guangyu Huang, Nick M. W. Roberts

claimed to represent "crustal rejuvenation", which was temporally defined as an influx of isotopically juvenile magma into an ancient crustal substrate (Mulder et al., 2021). Furthermore, this crustal rejuvenation is frequently considered to be the result of a geodynamic transition from stagnant-lid to mobile-lid tectonics in the early Mesoarchean (Bauer et al., 2020; Dhuime & Storey, 2012; Hartnady & Kirkland, 2019; Naeraa et al., 2012; Reimink et al., 2019). However, the onset timing of mobile-lid tectonics remains hotly disputed, with the proposal spanning from the Hadean to the late Archean (Cawood et al., 2018; Hawkesworth et al., 2020; Palin et al., 2020). Researchers often use diverse geological and geochemical records that yield mutually exclusive conclusions (e.g., C. B. Keller & Harrison, 2020; Tang et al., 2016). It has long been recognized that the Earth's mantle evolved from a relatively cool state to a hotter state from the Hadean to the early Mesoarchean (Herzberg et al., 2010; Korenaga, 2008). However, little attention has been paid to the role of mantle thermal evolution in contributing to continental crustal growth and evolution on the early Earth. Besides, whether this crustal rejuvenation was a global magmatic event during the early Mesoarchean still needs to be tested using igneous zircon Hf records in other cratonic blocks.

Considering the above controversies and uncertainties, we turn to the Yangtze Block, where several granitoid suites have recently been identified as emplaced during the early Mesoarchean, providing an excellent window to elucidate the evolution of Archean continental crust (Cui et al., 2021). Here, we focus on the Mesoarchean granitoids from the southwestern Yangtze Block. New geochemical and isotopic data, as well as thermodynamic modeling, constrain that the studied granitoids originated from isotopically juvenile crust. Statistical analysis further identified a step increase in mean zircon $\varepsilon Hf_{(t)}$ values at ca. 3.2–3.1 Ga, indicating that crustal rejuvenation is also present in the Yangtze Block during the early Mesoarchean. Based on the extant petrological and geochemical evidence, we posit a widespread crustal rejuvenation event across the Paleo-to Mesoarchean transition can be simply attributed to elevated mantle geotherms and possibly does not require a significant change in tectonic style.

2. Geological Background

As one of three Precambrian cratons, the South China Craton consists of the Yangtze Block in the northwest and the Cathaysia Block in the southeast (Figures 1a and 1b). The Archean basement rocks are mainly exposed in the Yangtze Block (Chen & Xing, 2016), including the Muzidian, Kongling, Zhongxiang, Yudongzi and Douling complexes in the northern part of the Yangtze Block (Guo et al., 2014; Tain et al., 2023; K. Wang et al., 2018; Zhou et al., 2018). Although the Paleo-Mesoproterozoic sedimentary units and igneous rocks have long been viewed as the oldest rocks in the southwestern Yangtze Block (Lu et al., 2019), the Cuoke complex with minor TTG rocks as old as ca. 3.1 Ga has been recently detected in the southwestern Yangtze Block (Figure 1b) (Cui et al., 2021; Zhao et al., 2020). The Cuoke complex mainly consists of early Paleoproterozoic granitoids with minor Archean igneous rocks (Cui et al., 2021). It is discontinuously exposed along several N-S and NE-SW trending ductile shear zones in the Cuoke area (Figure 1c) (Lu et al., 2021). Eleven granitoid samples were collected from the Archean units of the Cuoke complex (Figures 1d and 1f), of which two subgroups were further recognized based on their mineral assemblage. One group has the major mineral assemblage of quartz, plagioclase, and K-feldspar in variable proportions, with minor muscovite dispersed in the interstices between quartz and plagioclase (Figure 1e), whereas the other group mainly consists of quartz and plagioclase with minor secondary muscovite (Figure 1g). The granitoids collected from the Cuoke complex were analyzed for in situ zircon U-Pb-Hf-O isotopes, whole-rock geochemical, and Sm-Nd isotope analyses. In addition, statistical analysis of global data sets and thermodynamic modeling have further explored the continental crust evolution on the early Earth. The detailed descriptions of methods are depicted in the supplementary material (Text S1–S4 in Supporting Information S1, Tables S1–S8).

3. Results

The detailed descriptions of analytical results are depicted in Text S2 in Supporting Information S1. In brief, zircon grains from sample CK20-22 yield a crystallization age of 2,906 ± 16 Ma, which is slightly younger than sample CK20-28 (3,047 ± 34 Ma) (Figure S2 in Supporting Information S1). Both the 2.9 Ga and 3.05 Ga granitoids have high K/Na ratios (>0.3). However, the younger generation has relatively higher SiO_2 contents (75.7–74.4 wt.%), but lower Sr/Y ratios (1.8–1.1) and $\varepsilon Nd_{(t)}$ values (1.7–0.5) than the older generation (SiO_2 = 75.3–71.4 wt.%, Sr/Y = 13.9–4.3, $\varepsilon Nd_{(t)}$ = 3.1) (Figures 2a and 2b). Furthermore, the

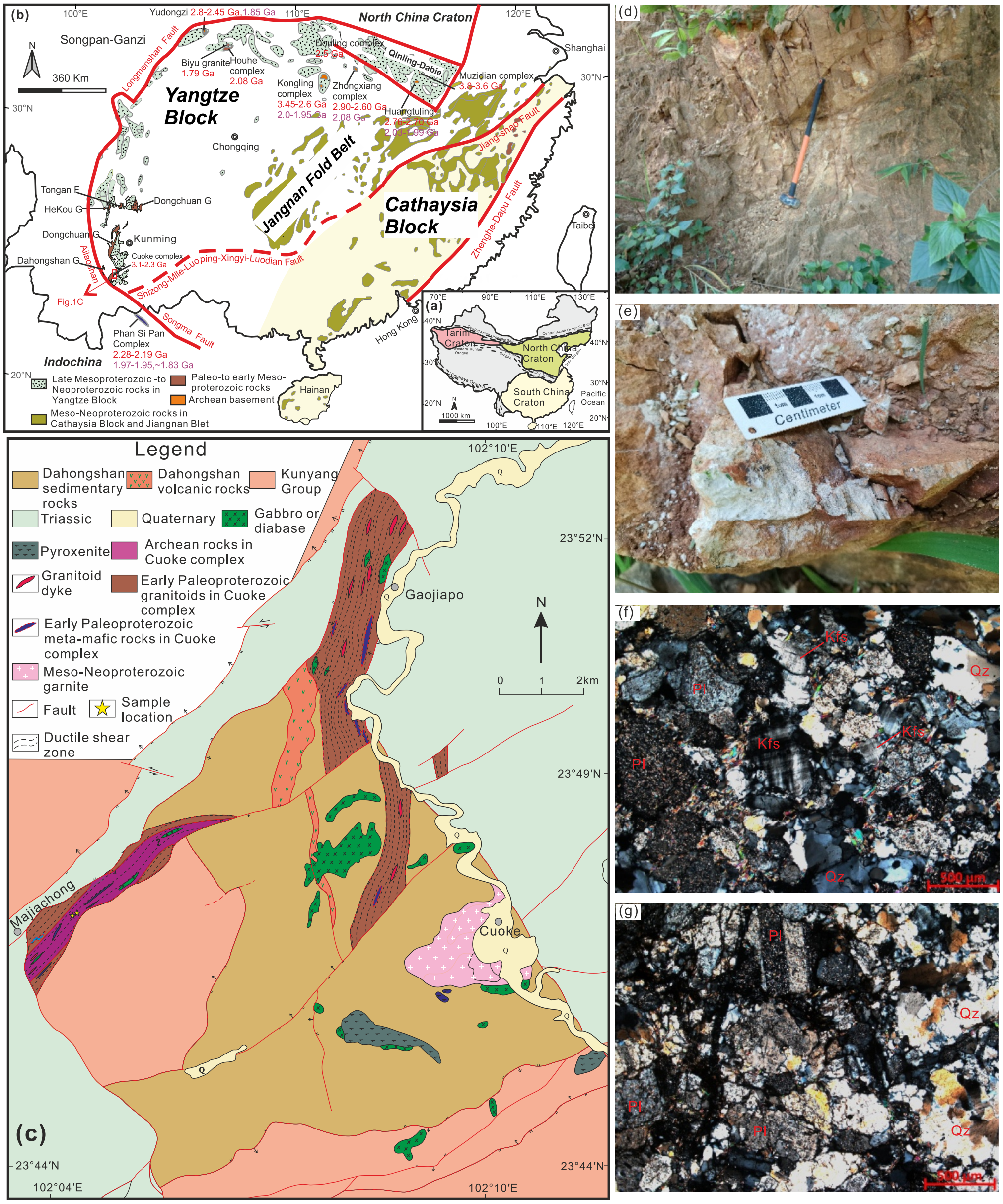

Figure 1. (a) Schematic tectonic framework of China showing three Precambrian cratons; (b) Overview of the Yangtze Block showing distribution of Archean and Paleoproterozoic basement rocks (after Lu et al. (2021)); (c) Geological map of the Cuoke area in the southwestern Yangtze Block (after Cui et al. (2021)); (d)–(g) Field and microscopic photographs of the studied granitoids. Abbreviations: Pl, plagioclase; Kfs, K-feldspar; Qz, quartz.

younger granitoids are classified as A-type granite based on their high 10,000*Ga/Al ratios (3.5–3.0) (Figure S5 in Supporting Information S1), while the older generation has elemental ratios and trace element distribution patterns resembling typical Archean potassic granite (Figures 2a and 2b, Figure S4 in Supporting Information S1). Herein, the 2.9 Ga and 3.05 Ga granitoids are termed A-type and potassic granite, respectively. The 2.9 Ga A-type granites have zircon $\delta^{18}O$ and $\varepsilon Hf_{(t)}$ values ranging from 6.7% ± 0.3% to 5.4% ± 0.2% and 5.8 ± 1.3 to 1.9 ± 1.2, respectively (Figure 2c, Table S3 and S4). In contrast, the 3.05 Ga potassic granites possess lower zircon $\delta^{18}O$ (5.7% ± 0.1% to 4.7% ± 0.3%) and $\varepsilon Hf_{(t)}$ values (5.2 ± 1.6 to −1.9 ± 1.3) (Figure 2c, Table S3 and S4).

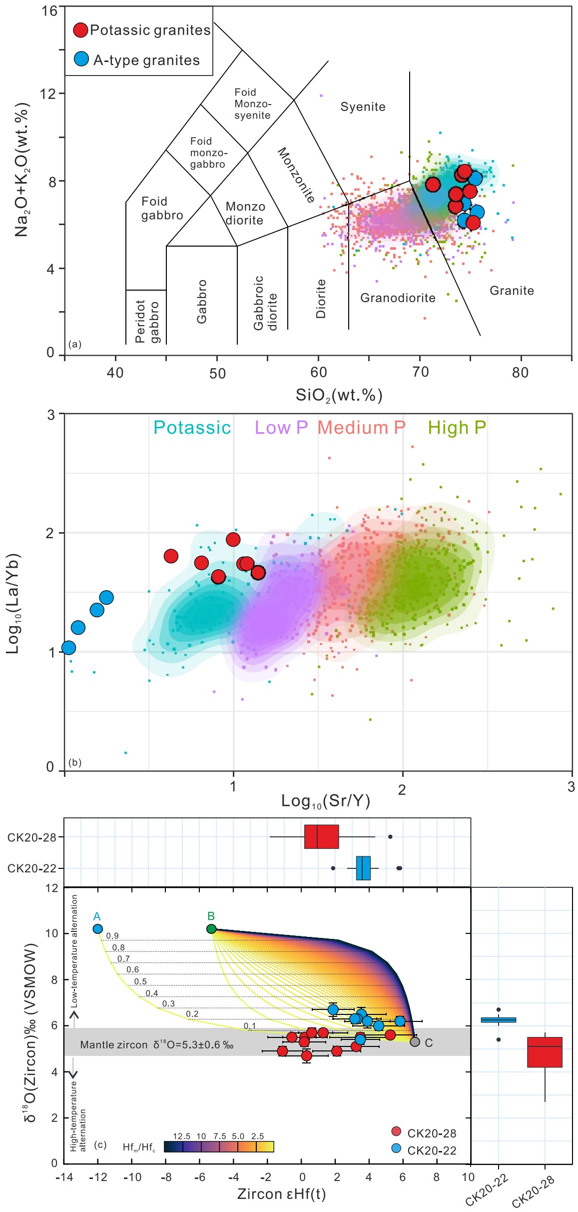

Figure 2. (a–b) Geochemical plots for the studied granitoids. Notes: The Archean potassic granites and high, middle, and low-pressure TTG rocks from Moyen (2011) are also plotted in the diagrams for comparison. Individual data points are superimposed on smoothed kernel density estimates. (c) plots of $\delta^{18}O$ versus $\varepsilon Hf_{(t)}$. Notes: ticks on the curves represent 10% mixing increments. A and B indicate crustal end-member 1 and 2 from Lu et al. (2021) with $\delta^{18}O = 10.2\%$, $\varepsilon Hf_{(t)} = -12$, and $\delta^{18}O = 10.2\%$, $\varepsilon Hf_{(t)} = -5.3$, respectively. C indicates the mantle end-member with $\delta^{18}O = 5.3\%$ (Valley et al., 2005), $\varepsilon Hf_{(t)} = 6.7$ (from depleted mantle $\varepsilon Hf_{(t)}$ values calculated at 3.0 Ga).

4. Discussion

4.1. Granitoid Petrogenesis

In general, granitic magmatism can be generated either by anatexis of preexisting crustal rocks with diverse lithologies or by extensive differentiation of mafic magma (Moyen, 2019). In the Ta/Sm versus Ta and Nb/Hf versus Nb diagrams, the studied granitoids display remarkably positive relationships, resembling the trend constructed by partial melting (Figure S6 in Supporting Information S1), thus arguing against their extensive differentiation origin. This deduction is partly supported by the field investigations, showing no contemporaneous mafic and intermediate rocks exposed in the SW Yangtze Block (Figure 1). In this situation, we suggest that the studied granitoids were most likely generated by anatexis of preexisting crustal rocks. The 2.9 Ga A-type granites from this study have supra-chondritic $\varepsilon Hf_{(t)}$ and $\varepsilon Nd_{(t)}$ values, suggesting their derivation from the isotopically juvenile crust. They have two-stage Hf model ages spanning from 2,975 to 3,215 Ma, further implying that the magma source was dominated by Mesoarchean juvenile igneous rocks. Additionally, they have primary zircon $\delta^{18}O$ values of 6.7% ± 0.3% to 5.4% ± 0.2%, indicating either mixing between mantle-derived juvenile magma and supracrustal materials altered by surface water under low-temperature (<300°C) conditions within the magma source area ("source" contamination) (Troch et al., 2020), or juvenile magma assimilating supracrustal materials during their emplacement ("path" contamination) (Cornet et al., 2022; Spencer et al., 2022). Although it is difficult to distinguish these two processes, simple two-end member mixing calculations constrain that around 10%–30% supracrustal materials are required to be incorporated into the juvenile magma to reconcile the Hf-O isotopic variations for the studied 2.9 Ga granitoids (Figure 2c). In contrast, undetectable supracrustal materials were involved in the genesis of 3.05 Ga potassic granites, given their normal mantle-like primary zircon $\delta^{18}O$ values (5.3 ± 0.6‰) (Valley et al., 2005). Furthermore, they possess slightly negative to positive $\varepsilon Hf_{(t)}$ and $\varepsilon Nd_{(t)}$ values with two-stage Hf model ages of 3,131–3,559 Ma, indicating that they originated from an isotopically juvenile Paleo-Mesoarchean crust. Considering that the studied granitoids have comparable zircon $\varepsilon Hf_{(t)}$ values with the contemporaneous TTG ($\varepsilon Hf_{(t)}$ = −2.5–7.5) exposed in the Cuoke area, thermodynamic modeling with a starting composition of the average composition of the Cuoke TTGs has been carried out (Zhao et al., 2020). The modeling results demonstrate that anatexis of the contemporaneous TTG under pressures of 0.4–2.0 GPa yields much lower SiO_2 contents and K/Na ratios compared with the studied granitoids (Figures S7a, b in Supporting Information S1). Consequently, the 3.05 Ga potassic granites are interpreted as the products of anatexis of a Paleo-Mesoarchean K-rich mafic crust. The studied granitoids display negative Eu anomalies (Figure S4 in Supporting Information S1), suggesting plagioclase either as a fractionating phase or as a residual mineral in their genesis. Additionally, the 3.05 Ga potassic granites have much lower HREE contents (La/Yb_N = 63–31) than the 2.9 Ga A-type granites (La/Yb_N = 21–8) (Figure S4 in Supporting Information S1), possibly reflecting a deeper crustal source for the former.

4.2. Widespread Crustal Rejuvenation Across the Paleo-Mesoarchean Transition

To explore the secular evolution of continental crust in the Yangtze Block, a Bayesian change-point algorithm was performed on an igneous zircon Lu-Hf isotopic data set compiled from Archean granitoids in the Yangtze Block. The statistical results show an increase in the mean zircon $\varepsilon Hf_{(t)}$ values at ca. 3.2–3.1 Ga from −1.95 to

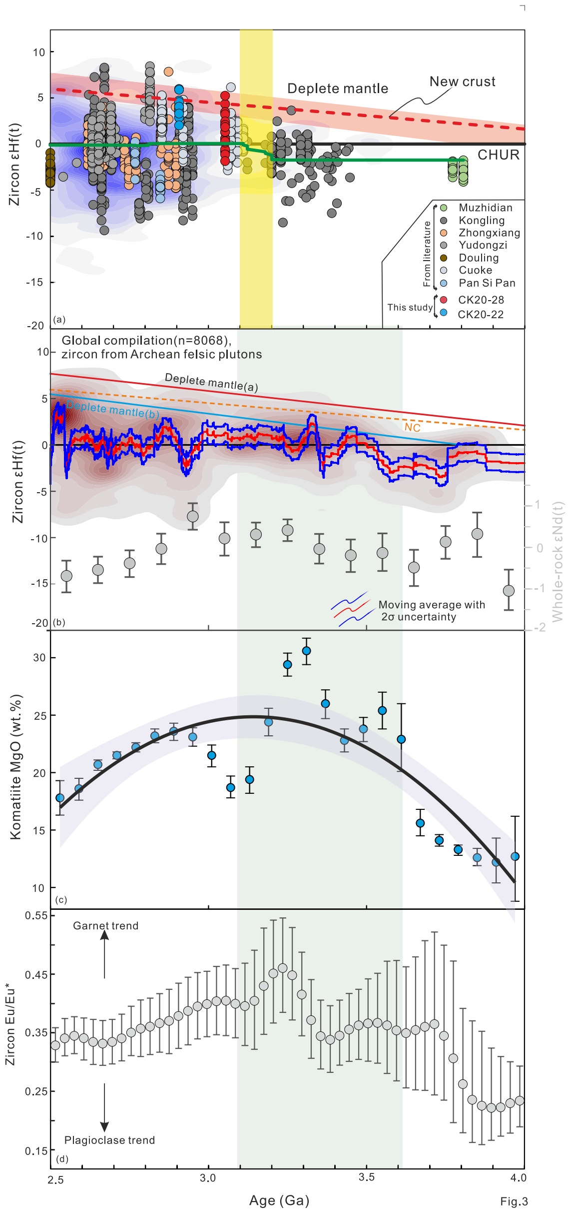

Figure 3. (a) Age versus zircon $\varepsilon Hf_{(t)}$. Notes: the blue "clouds" represent a bivariate kernel density estimate for collated detrital/xenocrystic zircon $\varepsilon Hf_{(t)}$ data (Table S7 in Supporting Information S1). The green line represents the results of Bayesian change point detection, showing a step increase of zircon $\varepsilon Hf_{(t)}$ at ca. 3.2–3.1 Ga; (b) Right panel: global mean $\varepsilon Nd_{(t)}$ contents in felsic rocks (Puetz & Condie, 2019); Left panel: bivariate kernel density estimate for collated magmatic zircon $\varepsilon Hf_{(t)}$ data of the Archean granitoids from the worldwide cratonic blocks (Table S7 in Supporting Information S1). The red curve represents the moving average analysis with 1σ uncertainties (blue curves); (c) Global mean MgO contents in komatiites from Tamblyn et al. (2023), the dark curve represents a polynomial fit with 95% confidence intervals; (d) Zircon Eu anomaly time series from 4.0 to 2.5 Ga. Notes: statistical methods utilized here are detailed in Text S5 in Supporting Information S1. The error bar is two standard error of the mean uncertainties determined after bootstrap resampling (C. B. Keller & Schoene, 2012).

−0.18 (Figure 3a). This isotopic variation reflects the addition of more juvenile materials to the Eo-Paleoarchean continental nuclei in the Yangtze Block during the early Mesoarchean. It is noteworthy that the detrital and igneous zircon compiled in the Yangtze Block have remarkably similar initial Hf isotopic variations from the Eoarchean to Neoarchean (Figure 3a), ruling out preservation bias issues for the igneous records (Hawkesworth et al., 2009). Furthermore, a moving average analysis was carried out on a globally compiled igneous zircon Lu-Hf isotopic data set, demonstrating supra-chondritic initial Hf isotopes marking the Paleo-Mesoarchean transition. These secular trends match well with supra-chondritic $\varepsilon Nd_{(t)}$ values for the contemporaneous felsic rocks (Figure 3b). In addition to this, a moderate increase in mean igneous zircon $\varepsilon Hf_{(t)}$ values also occurred at ∼3.9–3.8 Ga, consistent with detrital zircon from the Yilgarn Craton and Barberton Greenstone Belt (South Africa) featuring a step shift from sub-chondritic to supra-chondritic $\varepsilon Hf_{(t)}$ values at ∼3.8 Ga (Drabon et al., 2022; Mulder et al., 2021). However, the extant early Eoarchean igneous rocks on Earth dominantly possess zircon $\varepsilon Hf_{(t)}$ close to chondritic values, arguing against the presence of a depleted mantle and corresponding massive continental crust growth during the early Eoarchean (Fisher & Vervoort, 2018; Guitreau et al., 2012; Hiess & Bennett, 2016; Petersson et al., 2020), despite a more recent theoretical analysis disapproving of this proposal (Guo & Korenaga, 2023). These geological records plausibly imply insignificant crustal rejuvenation during the early Eoarchean (e.g., Reimink et al., 2023). In contrast, as we stated in the introduction section, numerous cratonic blocks registered a step increase in zircon $\varepsilon Hf_{(t)}$ values during the early Mesoarchean, demonstrating widespread crustal rejuvenation at that time. After 3.0 Ga, the igneous zircon yields vertical variation trends in $\varepsilon Hf_{(t)}$ time-space, indicating the concurrent generation of isotopically enriched and depleted felsic magma (Figures 3a and 3b), relating to both reworking of evolved crust and the addition of juvenile crust since that time (Bauer et al., 2020; Kirkland et al., 2021; Naeraa et al., 2012).

4.3. Induced Crustal Rejuvenation Due To Elevated Mantle Geotherms

Crustal rejuvenation across the Paleo-Mesoarchean transition has been increasingly discerned in various cratonic blocks based on igneous/detrital zircon Lu-Hf isotopic systematics (Bauer et al., 2020; Kirkland et al., 2021; Naeraa et al., 2012; Neil et al., 2023; Reimink et al., 2019; and this study). The prevailing model to account for this global magmatic event is a geodynamic transition from stagnant-lid to mobile-lid tectonics (possibly modern-style plate tectonics) on the early Earth (e.g., Bauer et al., 2020; Naeraa et al., 2012). However, the geodynamic regime for the early Earth is highly disputed (Brown et al., 2020; Cawood et al., 2018; Hawkesworth et al., 2020). One school argues that some form of subduction (e.g., mobile-lid tectonics) operated since the early Eoarchean (or even in the Hadean) (e.g., Arndt, 2023; Hastie et al., 2023). In contrast, the other workers favor the idea that the early Earth was dominated by stagnant-lid tectonics with different forms (e.g., heat-pipe, drips and plumes, delamination and upwellings, etc.) (e.g., Smithies et al., 2021; Stern, 2018; Tarduno et al., 2023), with a change to mobile-lid tectonics postulated to occur around the early Mesoarchean (e.g., Dhuime & Storey, 2012; Tang et al., 2016), even though this geodynamic shift in the early Mesoarchean has been questioned by other works based on different proxies (e.g., Greber et al., 2017; C. B. Keller & Harrison, 2020; Reimink et al., 2023).

Irrespective of these controversies, there is a consensus in the geoscience community that granitic rocks originate from mantle-derived basaltic rocks rather than from the direct melting of mantle peridotite (Clemens et al., 2020). It is widely noticed that the Archean granitoids possess whole-rock trace element compositions resembling Phanerozoic felsic rocks generated within subduction environments (Moyen, 2011). In contrast to this notion, Reimink et al. (2014) revealed that 4.02 Ga tonalitic gneiss within the Acasta Gneiss Complex in Canada has geochemical components analogous to sialic rocks from Iceland (Reimink et al., 2014). Indeed, previous experiments demonstrated that partial melting of primitive oceanic plateau yielded felsic melts with Eoarchean TTG-like geochemical compositions (Hastie et al., 2016). Moreover, the Paleo-to-Mesoarchean granitoids from classic dome-and-keel crust in the eastern Pilbara Craton are widely believed to be generated under a stagnant-lid regime (Smithies et al., 2021 and references therein). They have zircon grains with supra-chondritic $\varepsilon Hf_{(t)}$ values (e.g., Gardiner et al., 2017; Petersson et al., 2020), similar to those from subduction-related isotopically juvenile granitoids. In this situation, we have to acknowledge that the geochemical and zircon Hf isotopic compositions of the Archean granitoids merely record information associated with their magma source and magma evolution processes. As such, the observed shift in global zircon Hf isotopic records in the present study does not necessarily mean changes in geodynamics.

Arguably, significant rejuvenation of the Earth's continental crust requires a substantial influx of depleted mantle (e.g., Kirkland et al., 2021). Komatiites are generally considered to be the products of thermally hot mantle plumes (Herzberg, 2022). A bootstrap analysis of global komatiite compositions reveals a peak in MgO contents across the Paleo-Mesoarchean transition (Figure 3c), consistent with the high MgO contents in the contemporaneous basalts (B. Keller & Schoene, 2018). In addition, secular mantle cooling models with variable Urey ratios predict a maximum mantle temperature at that time (Korenaga, 2008). These lines of evidence indicate that both mantle plumes and the ambient mantle had anomalously elevated thermal states at the transitional time. Despite Ti-based zircon crystallization temperatures being controlled by a number of factors beyond temperature (Roberts et al., 2024; Siégel et al., 2018), it is also noteworthy that calculated zircon crystallization temperatures based on a compilation of detrital zircon trace elements show a gradual increase to a vertex during the early Mesoarchean (Figure S8 in Supporting Information S1). This potentially indicates that early Mesoarchean zircon crystallized from a hotter magma compared to zircon from prior and subsequent periods. Furthermore, Eu/Eu* in zircon has been argued to directly correlate to crustal thickness (Tang et al., 2020), although this correlation has also been questioned (Roberts et al., 2024; Triantafyllou et al., 2022; Yakymchuk et al., 2023). Using the same zircon trace element compilation (Table S8), we demonstrate that mean Eu/Eu* ratios peak during this Paleoarchean to Mesoarchean transition, with a secular trend resembling the MgO contents in global komatiites (Figure 3d). This may indicate that zircon from this transitional age crystallized from melts within the garnet stability field (i.e., thick crust) (e.g., Triantafyllou et al., 2022).

Collectively, with the foregoing geological and geochemical evidence in mind, we propose that the juvenile signal in the global zircon Hf isotopic data set across the Paleo-to-Mesoarchean transition indicates a flux of juvenile magma from the depleted mantle into the preexisting continental crust, with this flux relating to a peak in mantle temperatures. The elevated mantle geotherms would promote greater degrees of mantle melting leading to greater volumes of hot mafic and ultramafic magma pooling at the crust-mantle boundary. Subsequent partial melting or differentiation of these mantle-derived materials would yield geographically widespread granitoids with juvenile isotopic signatures injected into the preexisting ancient crust. This crustal rejuvenation would also promote thickening of the crust, leading to the continental crust gradually emerging above the seal level since the Mesoarchean (e.g., Chowdhury et al., 2021; Roberts & Santosh, 2018; W. Wang et al., 2022). In this scenario, we argue that the global crustal rejuvenation event across the Paleo-Mesoarchean transition results from slowly increasing mantle temperatures to the vertex rather than a short-term mantle overturn (Griffin et al., 2014). This is evidenced by gradual secular trends rather than evidence for short-lived events; however, it is difficult to prove the absence of mantle overturns, and these may have contributed to crust rejuvenation in some way. We also argue that the global crust rejuvenation can explain the observed changes in the igneous rock record and that these therefore do not require a geodynamic regime transition.

5. Conclusions

We use zircon U-Pb-Hf-O isotopes, whole-rock geochemical and Sm-Nd isotopic analysis to study the Mesoarchean granitic rocks from the SW Yangtze Block. Integrating our data with a global compiled zircon igneous Hf isotopes and igneous rocks geochemistry, the main conclusions of the study are summarized below:

~3.05 Ga potassic and ~2.9 Ga A-type granites from the SW Yangtze Block have depleted $\varepsilon Hf_{(t)}$ and $\varepsilon Nd_{(t)}$ values and nearly normal mantle-like zircon $\delta^{18}O$ values. Coupled with thermodynamic modeling, we suggested that the studied Mesoarchean granites were derived from isotopically juvenile crust.

A step increase in mean zircon $\varepsilon Hf_{(t)}$ values at 3.2–3.1 Ga has been detected in the compiled igneous zircon Lu-Hf isotopic data set from the Yangtze Block. In addition, a moving average analysis of global igneous zircon Lu-Hf isotopes compilation demonstrated supra-chondritic zircon $\varepsilon Hf_{(t)}$ values marking the Paleo-to Mesoarchean transition, suggesting widespread crustal rejuvenation at that time.

Integrated with the extant petrological and geochemical evidence, we contend that this global magmatic event can be simply explained by elevated mantle geotherms and does not necessitate a change in tectonic style. Thus, the thermal evolution of the mantle may have exerted a significant role in continental crust growth on the early Earth.

Conflict of Interest

The authors declare no conflicts of interest relevant to this study.

Data Availability Statement

The data supporting the conclusion of this study is available at Lu (2024).

Acknowledgments

We appreciate constructive comments from Prof. W. L. Griffin and an anonymous reviewer. We are also grateful to Prof. Fabio A. Capitanio and an anonymous Associate Editor for their effective handling of this manuscript. Mr. Bin Huang, Mr. Yang Zhang, and Prof. Xiao-Ping Xia are also thanked for their assistance during data acquisition. This study was co-supported by the National Natural Science Foundation of China (NSFC 42303013, 42288201, 42272228), and the China Post-doctoral Science Foundation (2023M733505). This is contribution No. IS-3489 from GIGCAS.

References

Arndt, N. (2023). How did the continental crust form: No basalt, no water, no granite. *Precambrian Research*, *397*, 107196. https://doi.org/10.1016/j.precamres.2023.107196

Bauer, A. M., Reimink, J. R., Chacko, T., Foley, B. J., Shirey, S. B., & Pearson, D. G. (2020). Hafnium isotopes in zircons document the gradual onset of mobile-lid tectonics. *Geochemical Perspectives Letters*, *14*, 1–6. https://doi.org/10.7185/geochemlet.2015

Brown, M., Johnson, T., & Gardiner, N. J. (2020). Plate tectonics and the Archean Earth. *Annual Review of Earth and Planetary Sciences*, *48*(1), 291–320. https://doi.org/10.1146/annurev-earth-081619-052705

Cawood, P. A., Hawkesworth, C. J., Pisarevsky, S. A., Dhuime, B., Capitanio, F. A., & Nebel, O. (2018). Geological archive of the onset of plate tectonics. *Philosophical Transactions: Mathematical, Physical and Engineering Sciences*, *376*(2132), 20170405. https://doi.org/10.1098/rsta.2017.0405

Chen, Z.-H., & Xing, G.-F. (2016). Geochemical and zircon U–Pb–Hf–O isotopic evidence for a coherent Paleoproterozoic basement beneath the Yangtze Block, South China. *Precambrian Research*, *279*, 81–90. https://doi.org/10.1016/j.precamres.2016.04.002

Chowdhury, P., Mulder, J. A., Cawood, P. A., Bhattacharjee, S., Roy, S., Wainwright, A. N., et al. (2021). Magmatic thickening of crust in non–plate tectonic settings initiated the subaerial rise of Earth's first continents 3.3 to 3.2 billion years ago. *Proceedings of the National Academy of Sciences*, *118*(46), e2105746118. https://doi.org/10.1073/pnas.2105746118

Clemens, J. D., Stevens, G., & Bryan, S. E. (2020). Conditions during the formation of granitic magmas by crustal melting—Hot or cold; drenched, damp or dry? *Earth-Science Reviews*, *200*, 102982. https://doi.org/10.1016/j.earscirev.2019.102982

Cornet, J., Laurent, O., Wotzlaw, J. F., Antonelli, M. A., Otamendi, J., Bergantz, G. W., & Bachmann, O. (2022). Reworking subducted sediments in arc magmas and the isotopic diversity of the continental crust: The case of the Ordovician Famatinian crustal section, Argentina. *Earth and Planetary Science Letters*, *595*, 117706. https://doi.org/10.1016/j.epsl.2022.117706

Cui, X. Z., Wang, J., Wang, X. C., Wilde, S. A., Ren, G. M., Li, S. J., et al. (2021). Early crustal evolution of the Yangtze Block: Constraints from zircon U-Pb-Hf isotope systematics of 3.1–1.9 Ga granitoids in the Cuoke Complex, SW China. *Precambrian Research*, *357*, 106155. https://doi.org/10.1016/j.precamres.2021.106155

Dhuime, B., Storey, C. D., & Cawood, P. A. (2012). A change in the geodynamics of continental growth 3 billion years ago. *Science*, *335*(6074), 1334–1336. https://doi.org/10.1126/science.1216066

Drabon, N., Byerly, B. L., Byerly, G. R., Wooden, J. L., Wiedenbeck, M., Valley, J. W., et al. (2022). Destabilization of long-lived Hadean protocrust and the onset of pervasive hydrous melting at 3.8 Ga. *AGU Advances*, *3*(2), e2021AV000520. https://doi.org/10.1029/2021av000520

Fisher, C. M., & Vervoort, J. D. (2018). Using the magmatic record to constrain the growth of continental crust—The Eoarchean zircon Hf record of Greenland. *Earth and Planetary Science Letters*, *488*, 79–91. https://doi.org/10.1016/j.epsl.2018.01.031

Gardiner, N. J., Hickman, A. H., Kirkland, C. L., Lu, Y., Johnson, T., & Zhao, J. X. (2017). Processes of crust formation in the early Earth imaged through Hf isotopes from the East Pilbara Terrane. *Precambrian Research*, *297*, 56–76. https://doi.org/10.1016/j.precamres.2017.05.004

Greber, N. D., Dauphas, N., Bekker, A., Ptáček, M. P., Bindeman, I. N., & Hofmann, A. (2017). Titanium isotopic evidence for felsic crust and plate tectonics 3.5 billion years ago. *Science*, *357*(6357), 1271–1274. https://doi.org/10.1126/science.aan8086

Griffin, W. L., Belousova, E. A., O'Neill, C., O'Reilly, S. Y., Malkovets, V., Pearson, N. J., et al. (2014). The world turns over: Hadean–Archean crust–mantle evolution. *Lithos*, *189*, 2–15. https://doi.org/10.1016/j.lithos.2013.08.018

Guitreau, M., & Blichert-Toft, J. (2014). Implications of discordant U–Pb ages on Hf isotope studies of detrital zircons. *Chemical Geology*, *385*, 17–25. https://doi.org/10.1016/j.chemgeo.2014.07.014

Guitreau, M., Blichert-Toft, J., Martin, H., Mojzsis, S. J., & Albarède, F. (2012). Hafnium isotope evidence from Archean granitic rocks for deep-mantle origin of continental crust. *Earth and Planetary Science Letters*, *337*, 211–223. https://doi.org/10.1016/j.epsl.2012.05.029

Guo, J.-L., Gao, S., Wu, Y.-B., Li, M., Chen, K., Hu, Z.-C., et al. (2014). 3.45 Ga granitic gneisses from the Yangtze Craton, South China: Implications for Early Archean crustal growth. *Precambrian Research*, *242*, 82–95. https://doi.org/10.1016/j.precamres.2013.12.018

Guo, M., & Korenaga, J. (2023). The combined Hf and Nd isotope evolution of the depleted mantle requires Hadean continental formation. *Science Advances*, *9*(12), eade2711. https://doi.org/10.1126/sciadv.ade2711

Hartnady, M. I. H., & Kirkland, C. L. (2019). A gradual transition to plate tectonics on Earth between 3.2 to 2.7 billion years ago. *Terra Nova*, *31*(2), 129–134. https://doi.org/10.1111/ter.12378

Hastie, A. R., Fitton, J. G., Bromiley, G. D., Butler, I. B., & Odling, N. W. A. (2016). The origin of Earth's first continents and the onset of plate tectonics. *Geology*, *44*(10), 855–858. https://doi.org/10.1130/g38226.1

Hastie, A. R., Law, S., Bromiley, G. D., Fitton, J. G., Harley, S. L., & Muir, D. D. (2023). Deep formation of Earth's earliest continental crust consistent with subduction. *Nature Geoscience*, *16*(9), 816–821. https://doi.org/10.1038/s41561-023-01249-5

Hawkesworth, C., Cawood, P., Kemp, T., Storey, C., & Dhuime, B. (2009). Geochemistry. A matter of preservation. *Science*, *323*, 49–50. https://doi.org/10.1126/science.1168549

Hawkesworth, C. J., Cawood, P. A., & Dhuime, B. (2020). The evolution of the continental crust and the onset of plate tectonics. *Frontiers in Earth Science*, *8*, 326. https://doi.org/10.3389/feart.2020.00326

Herzberg, C. (2022). Understanding the Paleoproterozoic Circum-Superior Large Igneous Province constrains the thermal properties of Earth's mantle through time. *Precambrian Research*, *375*, 106671. https://doi.org/10.1016/j.precamres.2022.106671

Herzberg, C., Condie, K., & Korenaga, J. (2010). Thermal history of the Earth and its petrological expression. *Earth and Planetary Science Letters*, *292*, 79–88. https://doi.org/10.1016/j.epsl.2010.01.022

Hiess, J., & Bennett, V. C. (2016). Chondritic Lu/Hf in the early crust–mantle system as recorded by zircon populations from the oldest Eoarchean rocks of Yilgarn Craton, West Australia and Enderby Land, Antarctica. *Chemical Geology*, *427*, 125–143. https://doi.org/10.1016/j.chemgeo.2016.02.011

Keller, B., & Schoene, B. (2018). Plate tectonics and continental basaltic geochemistry throughout Earth history. *Earth and Planetary Science Letters*, *481*, 290–304. https://doi.org/10.1016/j.epsl.2017.10.031

Keller, C. B., & Harrison, T. M. (2020). Constraining crustal silica on ancient Earth. *Proceedings of the National Academy of Sciences*, *117*(35), 21101–21107. https://doi.org/10.1073/pnas.2009431117

Keller, C. B., & Schoene, B. (2012). Statistical geochemistry reveals disruption in secular lithospheric evolution about 2.5 Gyr ago. *Nature*, *485*(7399), 490–493. https://doi.org/10.1038/nature11024

Kirkland, C. L., Hartnady, M. I. H., Barham, M., Olierook, H. K. H., Steenfelt, A., & Hollis, J. A. (2021). Widespread reworking of Hadean-to-Eoarchean continents during Earth's thermal peak. *Nature Communications*, *12*(1), 331. https://doi.org/10.1038/s41467-020-20514-4

Korenaga, J. (2008). Urey ratio and the structure and evolution of Earth's mantle. *Reviews of Geophysics*, *46*(2). https://doi.org/10.1029/2007rg000241

Lu, G. M. (2024). Supplementary materials for manuscript "Continental crust rejuvenation across the Paleo-Mesoarchean transition resulted from elevated mantle geotherms" [Dataset]. *Mendeley Data*. https://doi.org/10.17632/ygtzncvycr.1

Lu, G. M., Spencer, C. J., Tian, Y., & Wang, W. (2021). Significant increase of continental freeboard during the early Paleoproterozoic: Insights from metasediment-derived granites. *Geophysical Research Letters*, *48*(22), e2021GL096049. https://doi.org/10.1029/2021gl096049

Lu, G. M., Wang, W., Ernst, R. E., Söderlund, U., Lan, Z. F., Huang, S. F., & Xue, E. K. (2019). Petrogenesis of Paleo-Mesoproterozoic mafic rocks in the southwestern Yangtze Block of South China: Implications for tectonic evolution and paleogeographic reconstruction. *Precambrian Research*, *322*, 66–84. https://doi.org/10.1016/j.precamres.2018.12.019

Moyen, J. F. (2011). The composite Archaean grey gneisses: Petrological significance, and evidence for a non-unique tectonic setting for Archaean crustal growth. *Lithos*, *123*(1–4), 21–36. https://doi.org/10.1016/j.lithos.2010.09.015

Moyen, J. F. (2019). Archaean granitoids: Classification, petrology, geochemistry and origin. *Geological Society, London, Special Publications*, *489*(1), 15–49. https://doi.org/10.1144/sp489-2018-34

Mulder, J. A., Nebel, O., Gardiner, N. J., Cawood, P. A., Wainwright, A. N., & Ivanic, T. J. (2021). Crustal rejuvenation stabilised Earth's first cratons. *Nature Communications*, *12*(1), 3535. https://doi.org/10.1038/s41467-021-23805-6

Naeraa, T., Schersten, A., Rosing, M. T., Kemp, A. I., Hoffmann, J. E., Kokfelt, T. F., & Whitehouse, M. J. (2012). Hafnium isotope evidence for a transition in the dynamics of continental growth 3.2 Gyr ago. *Nature*, *485*(7400), 627–630. https://doi.org/10.1038/nature11140

Neil, B. J. C., Tersmette, D. B., Chacko, T., Heaman, L. M., Kjarsgaard, B. A., Martel, E., et al. (2023). Discovery of a giant 3.3–3.1 Ga terrane in the Rae craton, Canada: Implications for the timing and extent of ancient continental growth. *Geology*, *51*(6), 597–601. https://doi.org/10.1130/g51110.1

Palin, R. M., Santosh, M., Cao, W., Li, S. S., Hernández-Uribe, D., & Parsons, A. (2020). Secular metamorphic change and the onset of plate tectonics. *Earth-Science Reviews*, *207*, 103172. https://doi.org/10.1016/j.earscirev.2020.103172

Petersson, A., Kemp, A. I. S., Gray, C. M., & Whitehouse, M. J. (2020). Formation of early Archean Granite-Greenstone Terranes from a globally chondritic mantle: Insights from igneous rocks of the Pilbara Craton, Western Australia. *Chemical Geology*, *551*, 119757. https://doi.org/10.1016/j.chemgeo.2020.119757

Puetz, S. J., & Condie, K. C. (2019). Time series analysis of mantle cycles Part I: Periodicities and correlations among seven global isotopic databases. *Geoscience Frontiers*, *10*(4), 1305–1326. https://doi.org/10.1016/j.gsf.2019.04.002

Reimink, J. R., Chacko, T., Stern, R. A., & Heaman, L. M. (2014). Earth's earliest evolved crust generated in an Iceland-like setting. *Nature Geoscience*, *7*, 529–533. https://doi.org/10.1038/ngeo2170

Reimink, J. R., Davies, J. H. F. L., Moyen, J. F., & Pearson, D. G. (2023). A whole-lithosphere view of continental growth. *Geochemical Perspectives Letters*, *26*, 45–49. https://doi.org/10.7185/geochemlet.2324

Reimink, J. R., Pearson, D. G., Shirey, S. B., Carlson, R. W., & Ketchum, J. W. F. (2019). Onset of new, progressive crustal growth in the central Slave craton at 3.55 Ga. *Geochemical Perspectives Letters*, *10*, 8–13. https://doi.org/10.7185/geochemlet.1907

Roberts, N. M. W., & Santosh, M. (2018). Capturing the Mesoarchean emergence of continental crust in the Coorg Block, southern India. *Geophysical Research Letters*, *45*(15), 7444–7453. https://doi.org/10.1029/2018gl078114

Roberts, N. M. W., & Spencer, C. J. (2014). The zircon archive of continent formation through time. *Geological Society London Special Publications*, *389*(1), 27–32. https://doi.org/10.1144/sp389.14

Roberts, N. M. W., Spencer, C. J., Puetz, S., Keller, C. B., & Tapster, S. (2024). Regional trends and petrologic factors inhibit global interpretations of zircon trace element compositions. *EarthArXiv. Preprint*. https://doi.org/10.31223/X55D7R

Siégel, C., Bryan, S. E., Allen, C. M., & Gust, D. A. (2018). Use and abuse of zircon-based thermometers: A critical review and a recommended approach to identify antecrystic zircons. *Earth-Science Reviews*, *176*, 87–116. https://doi.org/10.1016/j.earscirev.2017.08.011

Smithies, R. H., Lu, Y., Kirkland, C. L., Johnson, T. E., Mole, D. R., Champion, D. C., et al. (2021). Oxygen isotopes trace the origins of Earth's earliest continental crust. *Nature*, *592*(7852), 70–75. https://doi.org/10.1038/s41586-021-03337-1

Spencer, C. J., Cavosie, A. J., Morrell, T. R., Lu, G. M., Liebmann, J., & Roberts, N. M. W. (2022). Disparities in oxygen isotopes of detrital and igneous zircon identify erosional bias in crustal rock record. *Earth and Planetary Science Letters*, *577*, 117248. https://doi.org/10.1016/j.epsl.2021.117248

Stern, R. J. (2018). The evolution of plate tectonics. *Philosophical Transactions of the Royal Society A: Mathematical, Physical and Engineering Sciences*, *376*(2132), 20170406. https://doi.org/10.1098/rsta.2017.0406

Tain, Y., Wang, W., Jin, W., Wu, Y. B., Wang, J., Deng, X., & Huang, S. F. (2023). Neoarchean granitic rocks from the Jiamiao area of the Dabie orogen: Implications on the formation and early evolution of the Yangtze Craton. *Science China Earth Sciences*, *65*(8), 1568–1585. https://doi.org/10.1007/s11430-021-9935-5

Tamblyn, R., Hermann, J., Hasterok, D., Sossi, P., Pettke, T., & Chatterjee, S. (2023). Hydrated komatiites as a source of water for TTG formation in the Archean. *Earth and Planetary Science Letters*, *603*, 117982. https://doi.org/10.1016/j.epsl.2022.117982

Tang, M., Chen, K., & Rudnick, R. L. (2016). Archean upper crust transition from mafic to felsic marks the onset of plate tectonics. *Science*, *351*(6271), 372–375. https://doi.org/10.1126/science.aad5513

Tang, M., Ji, W. Q., Chu, X., Wu, A., & Chen, C. (2020). Reconstructing crustal thickness evolution from europium anomalies in detrital zircons. *Geology*, *49*(1), 76–80. https://doi.org/10.1130/g47745.1

Tarduno, J. A., Cottrell, R. D., Bono, R. K., Rayner, N., Davis, W. J., Zhou, T., et al. (2023). Hadaean to Palaeoarchaean stagnant-lid tectonics revealed by zircon magnetism. *Nature*, *618*(7965), 531–536. https://doi.org/10.1038/s41586-023-06024-5

Triantafyllou, A., Ducea, M. N., Jepson, G., Hernández-Montenegro, J. D., Bisch, A., & Ganne, J. (2022). Europium anomalies in detrital zircons record major transitions in Earth geodynamics at 2.5 Ga and 0.9 Ga. *Geology*. https://doi.org/10.1130/G50720.1

Troch, J., Ellis, B. S., Harris, C., Bachmann, O., & Bindeman, I. N. (2020). Low-δ^{18}O silicic magmas on Earth: A review. *Earth-Science Reviews*, *208*, 103299. https://doi.org/10.1016/j.earscirev.2020.103299

Valley, J. W., Lackey, J. S., Cavosie, A. J., Clechenko, C. C., Spicuzza, M. J., Basei, M. A. S., et al. (2005). 4.4 billion years of crustal maturation: Oxygen isotope ratios of magmatic zircon. *Contributions to Mineralogy and Petrology*, *150*(6), 561–580. https://doi.org/10.1007/s00410-005-0025-8

Vervoort, J. D., & Kemp, A. I. S. (2016). Clarifying the zircon Hf isotope record of crust–mantle evolution. *Chemical Geology*, *425*, 65–75. https://doi.org/10.1016/j.chemgeo.2016.01.023

Wang, K., Li, Z.-X., Dong, S., Cui, J., Han, B., Zheng, T., & Xu, Y. (2018). Early crustal evolution of the Yangtze Craton, South China: New constraints from zircon U-Pb-Hf isotopes and geochemistry of ca. 2.9–2.6 Ga granitic rocks in the Zhongxiang Complex. *Precambrian Research*, *314*, 325–352. https://doi.org/10.1016/j.precamres.2018.05.016

Wang, W., Cawood, P. A., Spencer, C. J., Pandit, M. K., Zhao, J. H., Xia, X. P., et al. (2022). Global-scale emergence of continental crust during the Mesoarchean–early Neoarchean. *Geology*, *50*(2), 184–188. https://doi.org/10.1130/g49418.1

Wang, W., Spencer, C., Pandit, M. K., Wu, Y. B., Zhao, J. H., Zheng, J. P., et al. (2023). Crustal evolution and tectonomagmatic history of the Indian Shield at the periphery of supercontinents. *Geochimica et Cosmochimica Acta*, *341*, 90–104. https://doi.org/10.1016/j.gca.2022.10.040

Yakymchuk, C., Holder, R. M., Kendrick, J., & Moyen, J. F. (2023). Europium anomalies in zircon: A signal of crustal depth? *Earth and Planetary Science Letters*, *622*, 118405. https://doi.org/10.1016/j.epsl.2023.118405

Zhao, T. Y., Li, J., Liu, G. C., Cawood, P. A., Zi, J. W., Wang, K., et al. (2020). Petrogenesis of Archean TTGs and potassic granites in the southern Yangtze Block: Constraints on the early formation of the Yangtze Block. *Precambrian Research*, *347*, 105848. https://doi.org/10.1016/j.precamres.2020.105848

Zhou, G., Wu, Y., Li, L., Zhang, W., Zheng, J., Wang, H., & Yang, S. (2018). Identification of ca. 2.65 Ga TTGs in the Yudongzi complex and its implications for the early evolution of the Yangtze Block. *Precambrian Research*, *314*, 240–263. https://doi.org/10.1016/j.precamres.2018.06.011

References From the Supporting Information

Bell, E. A., Boehnke, P., & Harrison, T. M. (2016). Recovering the primary geochemistry of Jack Hills zircons through quantitative estimates of chemical alteration. *Geochimica et Cosmochimica Acta*, *191*, 187–202. https://doi.org/10.1016/j.gca.2016.07.016

Botev, Z. I., Grotowski, J. F., & Kroese, D. P. (2010). Kernel density estimation via diffusion. *Annals of Statistics*, *38*(5), 2916e2957. https://doi.org/10.1214/10-aos799

Brown, M. (2013). Granite: From genesis to emplacement. *Geological Society of America Bulletin*, *125*(7–8), 1079–1113. https://doi.org/10.1130/b30877.1

Gallagher, K., Bodin, T., Sambridge, M., Weiss, D., Kylander, M., & Large, D. (2011). Inference of abrupt changes in noisy geochemical records using transdimensional changepoint models. *Earth and Planetary Science Letters*, *311*(1–2), 182–194. https://doi.org/10.1016/j.epsl.2011.09.015

Green, E. C. R., White, R. W., Diener, J. F. A., Powell, R., Holland, T. J. B., & Palin, R. M. (2016). Activity–composition relations for the calculation of partial melting equilibria in metabasic rocks. *Journal of Metamorphic Geology*, *34*(9), 845–869. https://doi.org/10.1111/jmg.12211

Holland, T. J. B., & Powell, R. (2011). An improved and extended internally consistent thermodynamic dataset for phases of petrological interest, involving a new equation of state for solids. *Journal of Metamorphic Geology*, *29*(3), 333–383. https://doi.org/10.1111/j.1525-1314.2010.00923.x

Hoskin, P. W. O. (2005). Trace-element composition of hydrothermal zircon and the alteration of Hadean zircon from the Jack Hills, Australia. *Geochimica et Cosmochimica Acta*, *69*(3), 637–648. https://doi.org/10.1016/j.gca.2004.07.006

Jackson, S. E., Pearson, N. J., Griffin, W. L., & Belousova, E. A. (2004). The application of laser ablation-inductively coupled plasma-mass spectrometry to in situ U-Pb zircon geochronology. *Chemical Geology*, *211*, 47–69.

Li, J., Tang, S. H., Zhu, X. K., & Pan, C. X. (2017). Production and Certification of the Reference Material GSB 04-3258-2015 as a $^{143}Nd/^{144}Nd$ Isotope Ratio Reference. *Geostandards and Geoanalytical Research*, *41*(2), 255–262. https://doi.org/10.1111/ggr.12151

Li, X. H., Long, W. G., Li, Q. L., Liu, Y., Zheng, Y. F., Yang, Y. H., et al. (2010). Penglai zircon megacrysts: A potential new working reference material for microbeam determination of Hf–O isotopes and U–Pb age. *Geostandards and Geoanalytical Research*, *34*(2), 117–134. https://doi.org/10.1111/j.1751-908x.2010.00036.x

Li, X. H., Tang, G., Gong, B., Yang, Y., Hou, K., Hu, Z., et al. (2013). Qinghu zircon: A working reference for microbeam analysis of U-Pb age and Hf and O isotopes. *Chinese Science Bulletin*, *58*(36), 4647–4654. https://doi.org/10.1007/s11434-013-5932-x

Liu, Y. S., Gao, S., Hu, Z. C., Zong, K. Q., & Wang, D. B. (2010). Continental and oceanic crust recycling-induced melt–peridotite interactions in the Trans-North China Orogen: U–Pb dating, Hf isotopes and trace elements in zircons from mantle Xenoliths. *Journal of Petrology*, *51*(51), 392–399. https://doi.org/10.1093/petrology/egp082

Ludwig, K. R. (2003). *Isoplot v. 3.0: A Geochronological toolkit for Microsoft Excel*. Berkeley Geochronology Center.

Ma, Q., Zheng, J. P., Griffin, W. L., Zhang, M., Tang, H. Y., Su, Y. P., & Ping, X. Q. (2012). Triassic "adakitic" rocks in an extensional setting (North China): Melts from the cratonic lower crust. *Lithos*, *149*, 159–173. https://doi.org/10.1016/j.lithos.2012.04.017

Moyen, J. F., & Stevens, G. (2006). Experimental constraints on TTG petrogenesis: Implications for Archean geodynamics. In K. Benn, J. C. Mareschal, & K. C. Condie (Eds.), *Archean Geodynamics and Environments. Monographs* (pp. 149–178). AGU.

Pidgeon, R. T., Nemchin, A. A., & Whitehouse, M. J. (2017). The effect of weathering on U–Th–Pb and oxygen isotope systems of ancient zircons from the Jack Hills, Western Australia. *Geochimica et Cosmochimica Acta*, *197*, 142–166. https://doi.org/10.1016/j.gca.2016.10.005

Powell, R., & Holland, T. J. B. (1988). An internally consistent dataset with uncertainties and correlations: 3. Applications to geobarometry, worked examples and a computer program. *Journal of Metamorphic Geology*, *6*(2), 173–204. https://doi.org/10.1111/j.1525-1314.1988.tb00415.x

Qiu, X. F., Tong, X. R., Jiang, T., & Khattak, N. U. (2021). Reworking of Hadean continental crust in the Dabie orogen: Evidence from the Muzidian granitic gneisses. *Gondwana Research*, *89*, 119–130. https://doi.org/10.1016/j.gr.2020.08.014

Sawyer, E. W., Cesare, B., & Brown, M. (2011). When the continental crust melts. *Elements*, *7*(4), 229–234. https://doi.org/10.2113/gselements.7.4.229

Sláma, J., Košler, J., Condon, D. J., Crowley, J. L., Gerdes, A., Hanchar, J. M., et al. (2008). Plešovice zircon—A new natural reference material for U–Pb and Hf isotopic microanalysis. *Chemical Geology*, *249*(1–2), 1–35. https://doi.org/10.1016/j.chemgeo.2007.11.005

Sun, S. S., & Mcdonough, W. F. (1989). Chemical and isotopic systematics of ocean basalts: Implications for mantle composition and processes. In *Magmatism in the ocean basins* (Vol. 42(1), pp. 313–345). Geological Society London Special Publications.

Valley, J. W., Kita, N. T., & Fayek, M. (2009). In situ oxygen isotope geochemistry by ion microprobe. *MAC short course: Secondary ion mass spectrometry in the earth sciences*, *41*, 19–63.

Whalen, J. B., Currie, K. L., & Chappell, B. W. (1987). A-Type granites: Geochemical characteristics, discrimination and petrogenesis. *Contributions to Mineralogy and Petrology*, *95*(4), 407–419. https://doi.org/10.1007/bf00402202

White, R. W., & Powell, R. (2022). Melt loss and the preservation of granulite facies mineral assemblages. *Journal of Metamorphic Geology*, *20*(7), 621–632. https://doi.org/10.1046/j.1525-1314.2002.00206_20_7.x

White, R. W., Powell, R., Holland, T. J. B., Johnson, T. E., & Green, E. C. R. (2014). New mineral activity–composition relations for thermodynamic calculations in metapelitic systems. *Journal of Metamorphic Geology*, *32*(3), 261–286. https://doi.org/10.1111/jmg.12071

White, R. W., Powell, R., Holland, T. J. B., & Worley, B. A. (2000). The effect of TiO_2 and Fe_2O_3 on metapelitic assemblage at greenschist and amphibolite facies conditions: Mineral equilibria calculations in the system K_2O–FeO–MgO–Al_2O_3–SiO_2–H_2O–TiO_2–Fe_2O_3. *Journal of Metamorphic Geology*, *18*(5), 497–511. https://doi.org/10.1046/j.1525-1314.2000.00269.x

Wiedenbeck, M., Alle, P., Corfu, F., Griffin, W. L., Meier, M., Oberli, F., et al. (1995). Three natural zircon standards for U-Th-Pb, Lu-Hf, trace element and REE analyses. *Geostandards Newsletter*, *19*, 1–23. https://doi.org/10.1111/j.1751-908x.1995.tb00147.x

Wu, Y. B., & Zheng, Y. F. (2004). Genesis of zircon and its constraints on interpretation of U-Pb age. *Chinese Science Bulletin*, *49*(15), 1554–1569. https://doi.org/10.1007/bf03184122

Yang, Q., Xia, X. P., Zhang, W. F., Zhang, Y. Q., Xiong, B. Q., Xu, Y. G., et al. (2018). An evaluation of precision and accuracy of SIMS oxygen isotope analysis. *Solid Earth Sciences*, *3*(3), 81–86. https://doi.org/10.1016/j.sesci.2018.05.001